Mine Water Environ (2012) 31:242–251
DOI 10.1007/s10230-012-0188-2

TECHNICAL ARTICLE

Experimental Modelling of Chemical Clogging Processes in Dewatering Wells

Christoph Weidner · Sebastian Henkel · Stefanie Lorke · Thomas R. Rüde · Holger Schüttrumpf · Wiebke Klauder

Received: 2 December 2011 / Accepted: 15 May 2012 / Published online: 17 June 2012

Abstract An extensive array of deep, large diameter wells is required to locally dewater the aquifers in the Rhenish lignite mining district in Germany, some of which are anoxic. The performance of the wells is often influenced by the precipitation of metal hydroxides, such as FeOOH or MnOOH, which causes well clogging. A laboratory study was undertaken to gain a general understanding of the clogging processes and to create a basis for testing and developing techniques that could possibly prevent or reduce the loss of well efficiency. The chemical genesis of Fe-hydroxide incrustations in a well screen section was reproduced in an experimental model under controlled boundary conditions. In the model, the clogging process was accelerated by modifying the pH and Fe concentration relative to the in situ values. The effect of clogging on the hydraulic situation in the gravel material was quantified by measuring the hydraulic head in the section of the annular gravel pack. Increases in the hydraulic gradient up to 75 % were measured. Analysis of the gravel material using a sequential extraction procedure after the experiment yielded Fe contents up to 5.4 g kg^{-1}. According to X-ray diffraction, the incrustations mainly consist of 6 line ferrihydrite and lepidocrocite.

C. Weidner (✉) · T. R. Rüde
Institute of Hydrogeology, RWTH Aachen University,
Lochnerstr 4–20, 52064 Aachen, Germany
e-mail: weidner@hydro.rwth-aachen.de

S. Henkel · S. Lorke · H. Schüttrumpf
Institute of Hydraulic Engineering and Water Resources
Management (IWW), RWTH Aachen University,
Kreuzherrenstr 7, 52056 Aachen, Germany

W. Klauder
Water Resources Management, RWE Power AG,
Zum Gut Bohlendorf, 50935 Bergheim, Germany

Keywords Fe hydroxide incrustation · Chemical clogging · Well loss · Well ageing · Laboratory model · Open pit dewatering

Introduction

Mining in open pits in the Rhenish lignite district requires large-scale groundwater management and local dewatering of anoxic aquifers. Each year around 200 vertical dewatering wells with tubing diameters of up to 0.75 m are drilled to depths up to 750 m. More than 550 million m^3 of water are pumped by the mining company (RWE Power AG) every year and well ageing is an important factor (Fig. 1). One of the main aspects to be considered is the formation of iron oxide incrustations (ochre) in the gravel pack and well screen because this decreases well efficiency (Houben 2003). If a well affected by clogging cannot be regenerated, a new well must be drilled.

In contrast to wells drilled to supply drinking water, well operation in open pit mining aims to completely dewater all intersected aquifers above the coal seams near the open pit. Due to the low operating water level in wells for dewatering purposes, the well screens frequently fall dry, increasing the chance for the ambient air to reach anoxic groundwater. Additionally, the strong drawdown of the groundwater table leads to mixing of different groundwaters from several aquifer layers. Clogging effects generally occur if reduced groundwater with dissolved Fe(II) or Mn(II) ions is brought into contact with oxygen in the ambient air in the well tube (Holluta and Kölle 1964). The reduced metal ions oxidise to Fe(III) or Mn(IV), which are insoluble and therefore precipitate as oxide hydroxide minerals (Houben and Treskatis 2007).

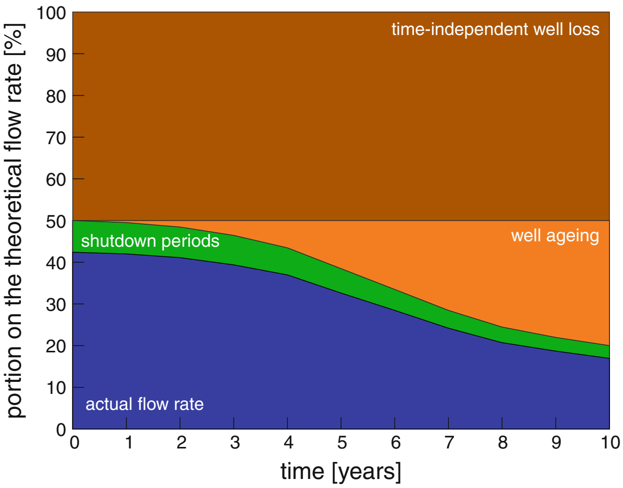

Fig. 1 Actual well capacity and contributions of the different causes of well loss (ageing, shutdown periods) on the theoretically achievable flow rate in a temporal dependency. The phrase "time-independent well loss" includes constructional influences, structurally disturbed ground, drilling mud cake and pressure losses at all passages in between the rock, gravel pack, screen pipe, and pump intake, whereas clogging accounts for the main part of "well ageing" (RWE Power AG, modified)

In this study, only clogging caused by Fe was considered. The most common Fe(III) oxide hydroxides and oxides are goethite (α-FeOOH), hematite (α-Fe_2O_3), ferrihydrite ($Fe_5HO_8 \cdot 4H_2O$), akaganéite (β-FeOOH), lepidocrocite (γ-FeOOH), and magnetite (Fe_3O_4, Cornell and Schwertmann 2003). Primary hematite only forms under elevated temperatures ($\approx$100 °C) and magnetite only forms under strongly alkaline conditions ($pH > 8$), so formation of these minerals is not expected (Cornell and Schwertmann 2003). The dominance of the other minerals is strongly controlled by the supply rate of Fe(II), with high reaction rates favouring the formation of ferrihydrite and lepidocrocite (because of their high solubility products). Ferrihydrites are thermodynamically metastable compounds and transform easily into goethite or hematite, so normally they are only found in rather young sediments (Childs 1992). As the incrustations in the model are quite young and are formed from a high supply of Fe(II), formation of ferrihydrite and/or lepidocrocite can be expected.

For considerations of the reaction kinetics, the equation for the simplest clogging reaction, the formation of FeO-OH, is consulted:

$$4Fe^{2+} + 6H_2O + O_2 \rightarrow 4FeOOH \downarrow + 8H^+ \qquad (1)$$

Adsorption of the precipitated minerals to all technical elements of the well system (gravel pack, well screen, pipes, and pump) results in a significant increase of well loss over time. The rate of the reaction is influenced by the pH and the concentrations of ferrous iron and oxygen (Houben and Treskatis 2007):

$$r = k_1 \frac{[Fe(II)] \cdot [O_{2,aq}]}{[H^+]^2} = k_1 [Fe(II)] \cdot [O_{2,aq}] \cdot 10^{2 \cdot pH} \qquad (2)$$

with r = reaction rate in mol L^{-1} min^{-1}; [Fe(II)] = concentration of dissolved ferrous iron in mol L^{-1}; $[O_{2,aq}]$ = concentration of dissolved oxygen in mol L^{-1}; $[H^+]$ = concentration of protons in mol L^{-1}; $k_1 = 1.515 \cdot 10^{-12}$ mol L^{-1} min^{-1}, after Davison and Seed (1983). Increasing the concentrations of Fe(II) and O_2 accelerates the reaction. Because the reaction produces protons, its rate also rapidly increases with rising pH (quadratic dependency on the proton concentration, Fig. 2). In addition, clogging in wells can be amplified by certain bacteria that use the conversion of dissolved Fe(II) to Fe(III) minerals as a source of energy (Hässelbarth and Lüdemann 1967; Ralph and Stephenson 1995; Rinck-Pfeiffer et al. 2000).

Methods

An experimental model of a well screen section (Fig. 3) was set up to reproduce the natural situation and processes under controlled boundary conditions (Rüde et al. 2010) so that the individual factors that affect the clogging process could be investigated separately. First, purely chemical clogging by iron oxides was considered.

In natural situations, the ageing process takes place over several years (cf. Fig. 1). In order to run the tests in an appropriate time frame, three aspects were consciously modified relative to natural conditions to accelerate the clogging process (cf. Eq. 2): the pH, the Fe(II) content, and

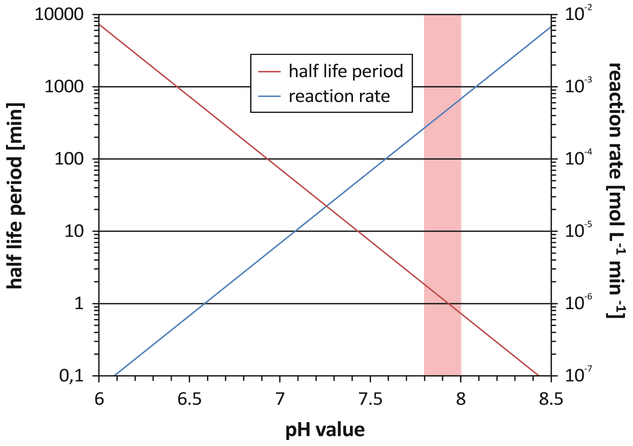

Fig. 2 Kinetics of the clogging reaction as a function of pH, expressed as reaction rate and half-life period (note the semi-logarithmic scale). For the calculations, the concentrations of Fe(II) and O_2 were assumed to be 40 mg L^{-1} and 2 mg L^{-1}, respectively, equalling the concentrations applied in the model. The *red* designation illustrates the pH range applied in the model to achieve a half-life period of the clogging reaction of about 1 min

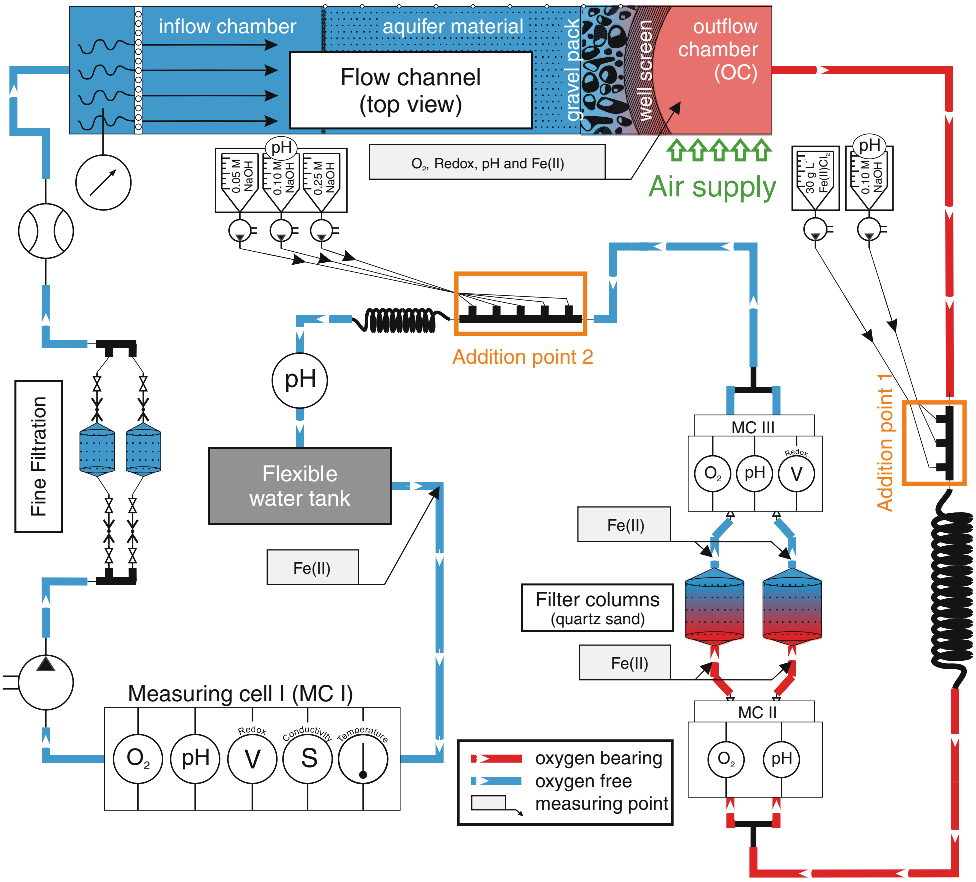

Fig. 3 Experimental setup with zones of O_2 bearing and O_2 free water in the circular flow system. During the test period each of the filter columns can be exchanged by a third one, whereas always only one of the fine filter columns at a time is integrated in the water cycle. A flexible water tank (150 L, Plastimo) is used as a storage reservoir for volume fluctuations and for buffering the chemical effects of addition point 2 by dilution. The spirals directly downstream of each addition point are static agitators with flow geometrical fittings

the active air supply. Natural waters from the open pits of the mining district usually have a pH of 6.7–7.2 and Fe(II) contents of 0–9 mg L^{-1} (RWE Power AG 2008), whereas in the model, a pH value of 7.8 and an Fe content between 40 and 80 mg L^{-1} were used. An active air supply raised the dissolved oxygen (DO) in the outflow chamber to about 1 mg L^{-1} or more. The appearance of biological/bacterial effects was prevented by two factors. First, the ferrous iron was added to the system using a solution of $FeCl_2$, causing the Cl^- content of the system water to continuously rise, thereby creating a hostile environment to bacteria. Second, an ultraviolet lamp (BLF111UVC by Berlan) was used to eliminate any remaining germs and bacteria in the water.

The experimental setup can be divided into two parts. The main part is the *flow channel*, where the experimental investigations were performed. The ancillary part is the *peripheral water cycle,* which is designated as a water processing chain to reprocess the water for the flow channel.

A section of a typical dewatering well in the Rhenish lignite mining district was installed in the *flow channel*. To simulate the natural situation, original aquifer material from the open pit Garzweiler in Germany was used. The aquifer material was taken from the Frimmersdorf Sand (horizon 6B, after Schneider and Thiele 1965), which forms a sandy interlayer in the main seam group of the upper Miocene Ville strata (Walter 2010). Horizon 6B separates the two coal seams Morken (Horizon 6A) in the lower bed and Frimmersdorf (Horizon 6C) in the upper bed (German Institute for Standardization 2001). The gravel pack and well screen were original well assembly materials, which were provided by RWE Power AG. In the flow channel, the water flows from left to right (Figs. 3, 4), first through the aquifer material, second through the gravel pack, third through the well screen and at last enters the uncovered outflow chamber. The walls of the channel consist of acrylic glass (PMMA), enabling an optical documentation of the clogging process.

The flow through the channel was controlled by pumps (Speck Pumpen Y-2951, regulated by electronic frequency converters FR-S520SE-0.4 k-EC by Mitsubishi Electrics) at the inflow and outflow to maintain a constant rate of 1.06 L min^{-1}. To simulate an infinite groundwater

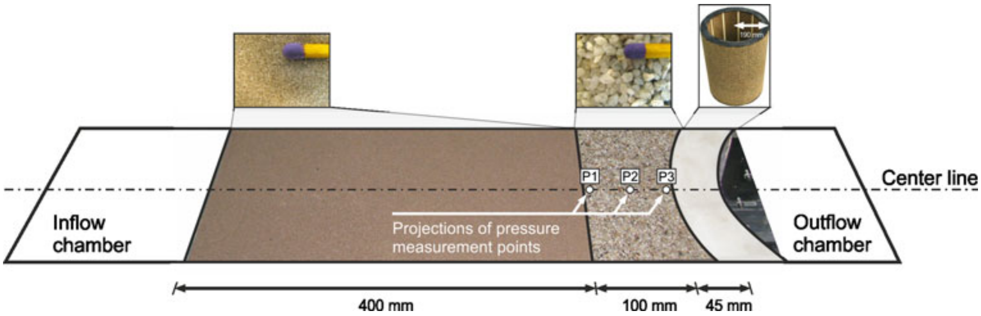

Fig. 4 Perspective top view of the flow channel with the aquifer material, gravel pack and well screen (height and breadth each 200 mm). Measuring points for pressure at the channel bottom are projected to the channel top for purposes of illustration (flow direction: *left* to *right*)

reservoir, the inflow chamber was kept under hydrostatic overpressure during the tests. Flow conditions change from confined to unconfined in the downstream part of the aquifer material due to the low water level in the outflow chamber, which was not covered. Thus, the water was in contact with the ambient air in the gravel pack, the well screen, and the outflow chamber, which is where the Fe(II) was oxidised.

In the *peripheral water cycle*, the discharge from the flow channel was continuously enriched with Fe(II) by addition of 1 mL min^{-1} of a 30 g L^{-1} Fe(II) solution of $FeCl_2 \cdot 4H_2O$ (p.a., Merck) at addition point 1 (Fig. 3) with a peristaltic proportioning pump (Ismatec Laboratoriumstechnik, BVP Standard). To prevent untimely oxidation and precipitation of Fe, the stock Fe(II) solution was acidified with 1 mL of HCl (25 %, p.a., Merck) per L of stock Fe(II) solution. The Fe(II) input was sufficient to chemically bond all of the residual oxygen that was not dissipated by the oxidation reaction in the flow channel. At this point, the water was also "re-enriched" with Fe to obtain a level between 40 and 80 mg L^{-1}. To maintain the oxidation reaction, the pH value had to be increased by continuous addition of NaOH (different concentrations, p.a., Merck). Behind addition point 1, the oxygen was entirely consumed by the formation of iron hydroxide or green rust I (Refait and Génin 1993), which were then filtered by columns of quartz sand (Quarzwerke GmbH, H4305-V, 0.5–1.0 mm). Subsequently, the pH value of the O_2-free water was adjusted to a level of 7.8 to ensure a constant high reaction rate in the channel outflow. To prevent the generation of green rust at this point in the system, which would have clogged the aquifer material at the channel inflow, the pH was not allowed to exceed a threshold value of 8. Green rust particles generated even below this threshold pH were removed by an additional fine filtration step directly upstream of the flow channel.

Physico-chemical parameters (pH, EC, DO and redox potential) were monitored at several locations in the model (WTW pH 320/330/340i, WTW Cond 340i, WTW Oxi 330/340i and WTW MultiLine P3 with probes WTW SenTix 41, WTW TetraCon 325, WTW CellOx 325 and Schott Redox Electrode BlueLine 31Rx). The measured values of redox potential given herein were converted to Eh by adding 217 mV. The Fe(II) concentration was determined spectrophotometrically (Dr. Lange CADAS 100) in irregular intervals using a pink Fe(II)-phenanthroline complex ($C_{12}H_8N_2 \cdot HCl \cdot H_2O$, p.a., Carl Roth), after the German Institute for Standardization (1983), to estimate the average Fe content of the gravel pack:

$$\mathrm{Fe_{tot}} = \frac{\Delta\,[\mathrm{Fe(II)}]\ \cdot \mathrm{Q} \cdot \mathrm{t}}{\mathrm{m}} = \frac{\left([\mathrm{Fe(II)}]_{\mathrm{MC\,I}} - [\mathrm{Fe(II)}]_{\mathrm{OC}}\right) \cdot \mathrm{Q} \cdot \mathrm{t}}{\mathrm{m}} \tag{3}$$

with Fe_{tot} = average Fe content of the gravel pack in g kg^{-1}; $\Delta[Fe(II)]$ = average decay of Fe(II) in the outflow chamber in mg L^{-1}; Q = flow rate in L min^{-1} (Q = 1.06 L min^{-1}, measured by flow meters DIGA 4 by Meister Strömungstechnik GmbH); t = total time of the experiment in h; m = mass of the gravel pack in kg (m ≈ 7 kg); $[Fe(II)]_{MC\ I}$ = average Fe concentration in the measurement cell I (MC I) in mg L^{-1}; $[Fe(II)]_{OC}$ = average Fe concentration in the outflow chamber (OC) in mg L^{-1}.

To quantify the progress of incrustation, the piezometric profile in the gravel pack was continuously monitored at three points using a high resolution pressure gauge device (cf. Fig. 4, Mecotec DP300-C). The dependency of the hydraulic gradient on the water level in the outflow chamber was first analysed with a low concentration of Fe(II) (<5 mg L^{-1}) to provide a reference test without any growth of Fe(III) hydroxide, but still with O_2-free water. The hydraulic regime of the gravel pack was characterised by calculating the Reynolds numbers:

$$\mathrm{Re_i(h_i)} = \frac{\mathrm{d_{eff}} \cdot \mathrm{v_i}}{\nu_{\mathrm{kin}}} = \frac{\mathrm{d_{eff}} \cdot \mathrm{Q}}{\nu_{\mathrm{kin}} \cdot \mathrm{A_i}} = \frac{\mathrm{d_{eff}} \cdot \mathrm{Q}}{\nu_{\mathrm{kin}} \cdot \mathrm{b_{channel}} \cdot \mathrm{h_i}} \tag{4}$$

with Re_i = Reynolds number at measuring point i; h_i = water level in mm at measuring point i; d_{eff} = effective grain size in mm (here d_{eff} = 1.672 mm, Klauder 2011); ν_{kin} = kinematic viscosity of the process water in $m^2\ s^{-1}$ ($\nu_{kin} = 1.139 \cdot 10^{-6}\ m^2\ s^{-1}$ at T = 15 °C); v_i = Darcy velocity in m s^{-1} at measuring point i; Q = system flow in L min^{-1} (Q = 1.06 L min^{-1});

A_i = flow-effective cross-section area in mm^2 at measuring point i; $b_{channel}$ = channel breadth in mm ($b_{channel}$ = 200 mm).

After finishing the reference test, the Fe(II) content was increased to a level between 40 and 80 mg L^{-1} to perform the clogging experiment. The same water levels in the outflow chamber were applied as in the reference situation. The comparison of the hydraulic gradient of the reference and the clogging situation was used to quantify the influence of incrustations on the hydraulic situation.

After the test was finished, the gravel pack material was excavated in 2 cm layers. Each layer was photographed and sampled. The samples were analysed by a sequential extraction procedure (SEP) focusing on poorly-crystallised and well-crystallised iron hydroxides (fractions 3 and 4, after Wenzel et al. 2001). Total organic carbon (TOC) was measured to prove the absence of biological clogging effects. For measurements of X-ray diffraction (XRD), the samples were treated either by an ultrasonic bath (Bandelin Sonorex Super RK 106) or by a magnetic stirrer (IKA-COMBIMAG-RCT) to redisaggregate the fine-grained Fe-hydroxide particles from the coarse-grained filter gravel. The two grain classes were then separated by wet sieving (Haver & Boecker analysis sieve 1 mm) to enrich the precipitates of the clogging process in the fine fraction and thus allow us to mineralogically characterise these precipitates separately from the coarse grains of the original gravel pack (96 % quartz, 4 % orthoclase). The fine fraction was dried and milled to a submicrometer particle size using a McCrone micronizing corundum mill. The XRD-measurements were conducted by the Institute of Mineralogy of the Freiberg University of Mining and Technology and interpreted by Rietveld mineral phase analysis using BGMN software (Bergmann et al. 1998) with the structure file database of the Institute of Clay and Interface Mineralogy of RWTH Aachen University. For comparison, the same procedures were applied to a natural sample from the field, taken at an excavated well in the open pit Garzweiler.

Results and Discussion

The continuous measurements (Table 1) show the system to be free of dissolved oxygen except for the outflow chamber. The high value at point MC III is obviously due to a drift in the zero value of the O_2 probe, as there was a low O_2 content at point MC II and no additional source of oxygen between MC II and MC III. In the outflow chamber (OC), the redox potential rises rapidly from Eh = −384 mV to around Eh = 246 mV due to the oxygen input. The Fe(II) content and the pH in the outflow chamber decrease in response to the clogging reaction. The specific electrical conductivity rose continuously from the beginning of the experiment due to the continuous addition of the $FeCl_2$ solution. Over the 176 h duration of the experiment, this results in a mean specific electrical conductivity of 4.3 mS cm^{-1}. However, the number of pH and Eh values in the outflow chamber were quite low due to the manual recording of values; in future experiments, these will also be logged automatically.

Table 1 Long term arithmetic means (m), standard deviations (s) and value numbers (n) of dissolved oxygen concentration (DO), pH value (pH), redox potential (Eh), electrical conductivity (EC) and dissolved concentration of ferrous iron (Fe(II)) of the latest experiment, measured either automatically (Auto) or manually (Man) at the points in the model defined in Fig. 3, k = 1,000

Parameter	Unit	Point	m	s	n	Mode
DO	[mg L^{-1}]	OC	1.03	0.51	243 k	Auto
		MC II	0.17	0.12	20	Man
		MC III	0.95	0.13	24	Man
pH	[-]	OC	6.85	0.48	10	Man
		MC II	8.05	0.21	24	Man
		MC III	7.63	0.18	24	Man
		bA2	7.82	0.09	243 k	Auto
		MC I	7.90	0.04	243 k	Auto
Eh	[mV]	OC	246	100	10	Man
		MC I	−384	7.2	243 k	Auto
EC	[mS cm^{-1}]	MC I	4.31	0.05	243 k	Auto
Fe(II)	[mg L^{-1}]	OC	58.5	17.7	78	Man
		MC II	63.1	19.1	82	Man
		MC III	63.8	18.3	163	Man
		MC I	62.4	16.4	78	Man

The growth of incrustations at seven distinct test times is shown in Fig. 5. The first picture shows the situation shortly after Fe(II) addition began. It was clear that the clogging reaction only takes place in the vadose zone of the gravel pack. The concentration of dissolved oxygen was apparently too low in the phreatic zone to produce visible incrustations and of course, no Fe(II) bearing water was available in the upper part of the vadose zone. The first picture also shows that there was an obvious vertical flow component and a higher influence of capillarity near the interface between aquifer material and gravel pack, allowing the incrustations to nearly reach the top of the flow channel.

The following pictures show the effects of the water level in the outflow chamber, which was consciously raised in 20 mm steps to include the complete gravel pack in the clogging process and to investigate the effect of the water level on the hydraulic situation. The same water levels were applied in the clogging experiment as in the reference situation to allow a comparison of both situations.

Using the total time of the clogging experiment, t = 176 h, and the difference in average Fe(II)

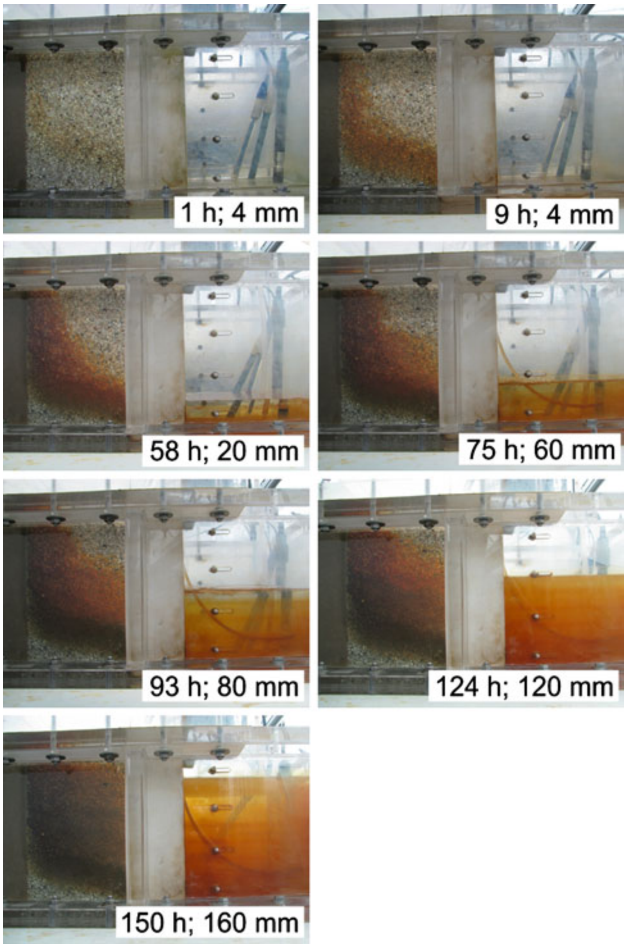

Fig. 5 Progress of incrustation growth in the gravel pack. Front view of aquifer material, gravel pack, screen pipe section and outflow chamber (*left* to *right* of each picture; *height* 200 mm). The numbers indicate the experimental duration in hours and the water level in the outflow chamber in mm at the time the pictures were taken

concentrations at points MC I and OC [cf. Fig. 3; Table 1: $\Delta[\mathrm{Fe(II)}] = 3.9\ \mathrm{mg\ L^{-1}}$ (62.4–58.5 $\mathrm{mg\ L^{-1}}$)], the average Fe content in the gravel pack was estimated from Eq. 3 to be $\mathrm{Fe_{tot}} = 6.24\ \mathrm{g\ kg^{-1}}$. In a previous experiment, before the fine filtration was installed directly upstream of the flow channel, it was not possible to differentiate between green rust precipitated in the inflow chamber and Fe(III) hydroxides in the gravel pack. Thus, the Fe balance yielded an overestimation of about 10 g of Fe per kg gravel material ($t = 295$ h, Weidner et al. 2011).

From Eq. 4, the Reynolds numbers were calculated at all three cross sections in the gravel pack for all 11 water levels of the reference test (Fig. 6). The evaluations show that at water levels higher than 120 mm (the highest water level possible in the model is 200 mm), the Reynolds numbers were below $\mathrm{Re} = 1$, implying linear laminar flow conditions. At lower water levels, Re exceeded 1, indicating a transition from a laminar to turbulent flow regime ($1 < \mathrm{Re} < 100$, Klauder 2011). It was also observed that above $\mathrm{Re} = 1$, the Re numbers were affected by where they were measured. The nearer the measurement was to the outflow chamber, the higher the Re number, due to the decreasing flow-effective cross-section area and the associated increasing flow velocity.

Pressure losses were calculated for all three possible combinations of the three points for pressure measurements during the reference test and during the clogging experiment. The arithmetic mean of all measurements was derived for each water level in the outflow chamber. Comparing the pressure losses in the reference situation with those in the clogging situation reveals a clear increase in pressure loss that was due to the clogging progress (Fig. 7). All three data series were calculated from direct measurements, although the pressure losses between P1 and P3 correspond rather well to the sum of the other two combinations. The increase in pressure loss at the lowest water level (around 4 mm) was less than at the other water levels, because at this level, only the upper part of the gravel pack (i.e. the vadose zone, which is not as flow effective as the lower phreatic zone) is affected by clogging. Then, when the water level is raised, the former vadose zone becomes part of the new phreatic zone, which is already affected by the clogging process.

The clogging processes increased pressure loss in the gravel pack by up to 75 % (Table 2), whereas in a previous experiment, which was focused on the hydrochemical rather than the hydraulic situation, an increase of up to 30 % was estimated (Weidner et al. 2011).

For the sequential extraction procedure, different zones of the gravel pack were sampled, based on the colour of the gravel (Fig. 8). During this 176 h experiment, total Fe contents of the sampled locations showed values up to $\mathrm{Fe_{tot}} = 5.36\ \mathrm{g\ kg^{-1}}$ (point 9, Table 3), somewhat less than the average content predicted by the Fe balance ($6.24\ \mathrm{g\ kg^{-1}}$, see calculation above). The values more or less correlate with the observed degree of staining and the colour intensity. In a previous experiment with $t = 295$ h, maximum contents of up to $\mathrm{Fe_{tot}} = 15\ \mathrm{g\ kg^{-1}}$ were reached (Henkel et al. 2012). The percentage of well-crystallised Fe(III) minerals in all 14 samples ranged from 11 to 99 %, and averaged 70 %, showing that the incrustations already have apparently reached a certain degree of crystallinity. This assumption is confirmed by the XRD measurements (Fig. 9).

Figure 9a shows that due to their low content, Fe-minerals in the gravel material cannot be detected directly. Both described methods were successful in enriching the $\mathrm{Fe_{tot}}$ content of the sample. Using the magnetic stirrer (Fig. 9b), besides the iron oxides (lepidocrocite and 6 line ferrihydrite), also orthoclase (originating from the initial gravel material) was enriched relatively to quartz.

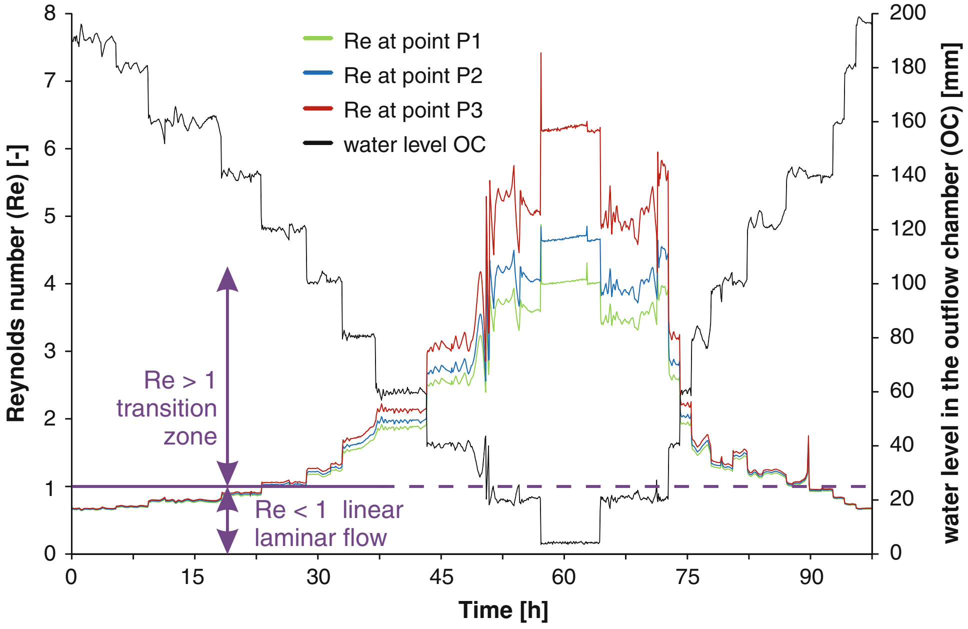

Fig. 6 Evaluation of the Reynolds numbers at the three cross sections (three pressure measurement points cf. Fig. 4) in the gravel pack during the reference test in dependence of the water level in the outflow chamber. The water level at first is stepwise lowered and then raised again

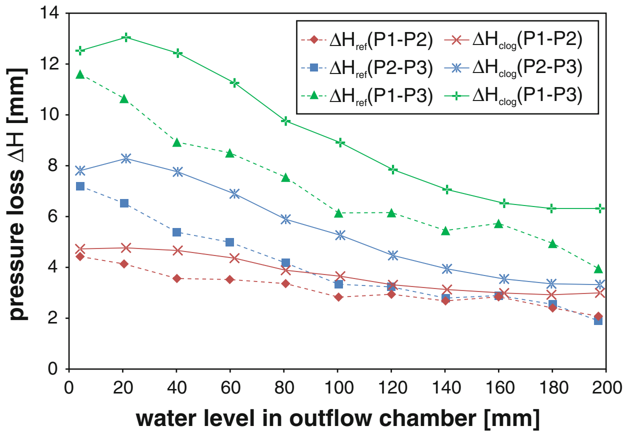

Fig. 7 Evaluation of the pressure losses in the gravel pack for all combinations of the three pressure measurement points (cf. Fig. 4) versus water level in the outflow chamber. The gradients in the clogging experiment (*clog*) are compared to the gradients in the reference situation (*ref*)

Table 2 Percental increase of pressure losses in the clogging experiment relative to the reference situation for all three combinations of measuring points P1, P2 and P3 versus water level in the outflow chamber

Water level (mm)	Increase of pressure loss (%)		
	P1–P2	P2–P3	P1–P3
197.2	42.8	75.1	59.8
180.1	21.7	31.8	27.7
160.0	5.3	22.4	18.3
140.2	46.7	41.2	29.6
120.1	12.6	38.4	27.5
100.4	29.0	58.0	45.1
80.7	15.7	41.2	29.3
59.9	23.9	38.2	32.4
40.2	30.9	44.1	39.2
20.5	15.3	27.0	22.6
4.1	6.8	8.5	7.9

Orthoclase enrichment was considerably less with the ultrasonic bath (Fig. 9c; Table 4). The higher background in the measurements of the enriched samples accounts for the higher content of X-ray-amorphous minerals like poorly-crystallised Fe hydroxides. The high content of lepidocrocite and the formation of 6 line ferrihydrite, rather than 2 line ferrihydrite, show that the incrustations have already reached a significant degree of crystallinity. In the natural sample from the open pit Garzweiler, a high content of 6 line ferrihydrite was detected after enrichment by the ultrasonic bath (Fig. 9d). However, no lepidocrocite or other Fe(III)-minerals, including goethite, hematite, akaganéite, and magnetite could be detected in this sample, indicating a lower degree of crystallinity of the Fe-minerals. The original Fe contents were $Fe_{tot} = 12.1$ g kg^{-1} (27 % well crystallised) in the sample from the model and $Fe_{tot} = 30.9$ g kg^{-1} (3 % well crystallised) in the sample from the field.

The total organic carbon (TOC) content of one solidified sample from the gravel pack of the model with $Fe_{tot} = 3.4$ g kg^{-1} (46 % well crystallised) showed a value of TOC = 0.035 wt.%, whereas a sample of fresh gravel material contained 0.026 wt.% TOC. Thus, the increased loss of pressure as well as the solidification of the sample is certainly not an effect of some kind of biological process, but due to the growth of Fe incrustations.

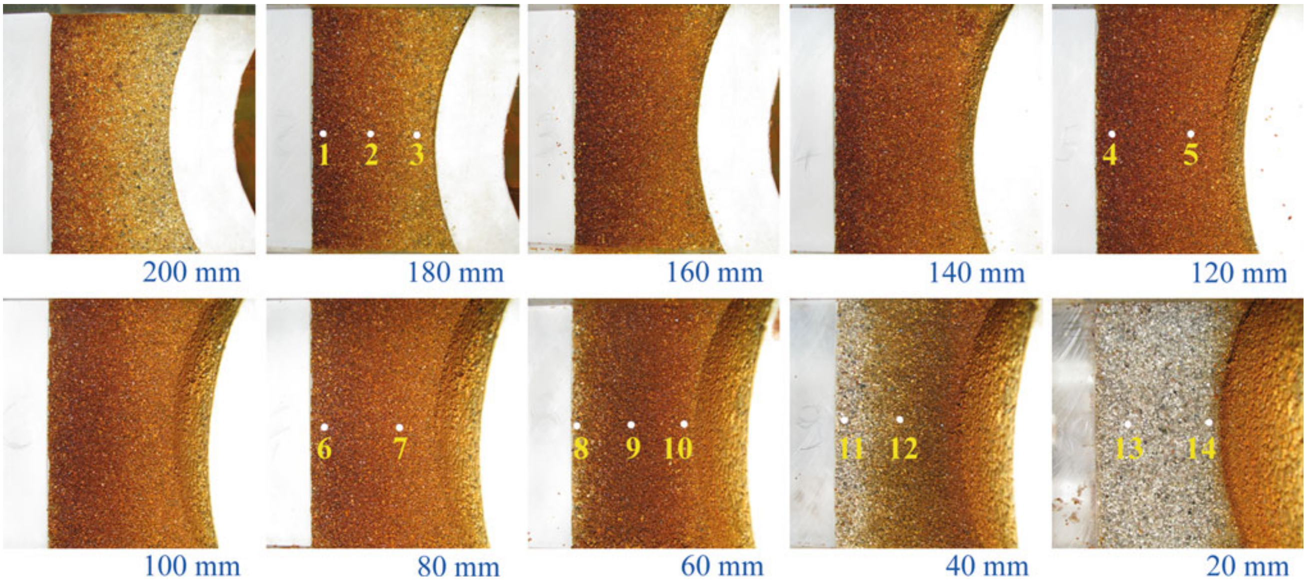

Fig. 8 Layers of gravel pack material after the clogging experiment. The thickness of each layer is 20 mm, while its height above the channel bottom is indicated by *blue labels*. *White dots* with *yellow numbers* indicate sampling locations for SEP-analysis

Table 3 Results of SEP-analysis in terms of total Fe content (Fe_{tot}) and well-crystalline fraction (fraction 4 after Wenzel et al. 2001) as percentage of the total content

No	Fe_{tot} (g kg^{-1})	Crystalline (%)
1	2.56	62
2	1.78	81
3	0.30	60
4	5.19	77
5	1.79	99
6	2.14	81
7	3.62	99
8	0.65	32
9	5.36	99
10	1.23	95
11	0.07	97
12	0.23	73
13	0.47	11
14	0.33	18

Conclusions and Prospect

The laboratory reproduction of the chemical clogging process was successful. A significant decrease in the hydraulic conductivity of the gravel pack was reached in less than 176 h. Thus, acceleration of the process seems to have worked quite well and the tests could be accomplished in an appropriate time frame. The clogging reaction only took place in the outflow chamber of the flow channel and was due to incrustations of Fe minerals. This was confirmed optically as well as with hydrochemical measurements. The possibility of biologically induced mineral precipitation was excluded by the TOC measurements.

Most of the incrustation took place in the vadose zone of the gravel pack since the diffusion of oxygen through the water was too slow to allow significant oxidation below that level, given the strong flow rate. Changing the water level in the outflow chamber over the entire possible range generated a more homogeneous distribution of incrusted areas but was time consuming and caused flow in the gravel pack to reach the upper threshold of the linear laminar flow regime. In future experiments, the hydraulic gradient should be measured at just one or two water levels in the outflow chamber with $Re < 1$ to precisely evaluate the time dependency of the pressure loss induced by the clogging process, instead of considering effects of the water level. The clogging affinity of a specific setting of the well model can then be evaluated by how fast a certain pressure loss is observed.

Although the Fe content in the gravel pack barely reached 0.5 wt.%, the hydraulic gradient increased by 75 %. Given the high volume of Fe minerals required to clog the pore volume of the gravel pack, the precipitated Fe minerals must be of fairly low density. Mineralogical analysis showed that ferrihydrite was the main mineral formed during the clogging process. The water content and density of ferrihydrite can vary very widely; the ferrihydrite formed in this experiment seems to have a high water content. In contrast to a field sample, lepidocrocite also formed in the model, indicating that the clogging process in

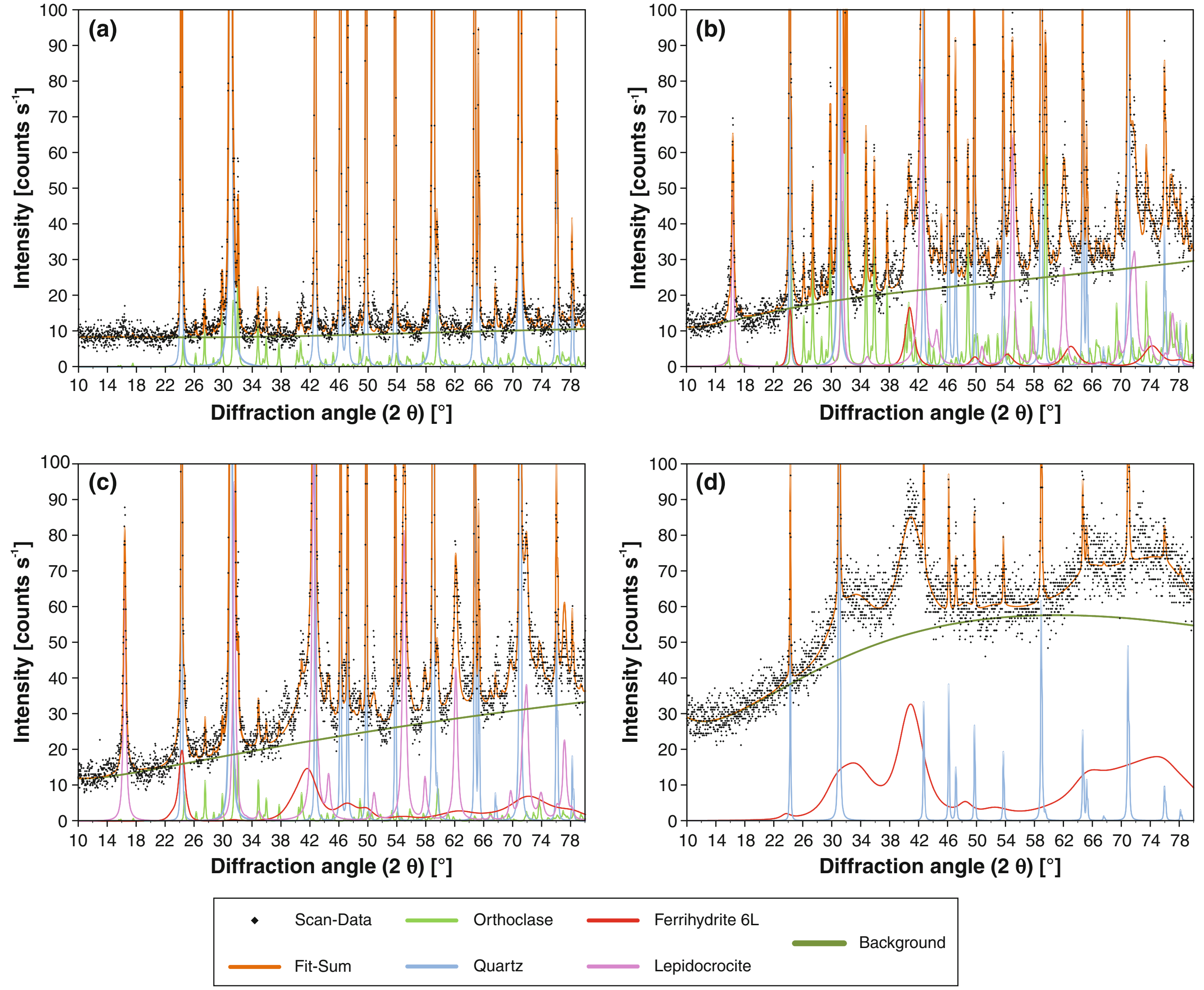

Fig. 9 XRD-scans of one sample from the model. **a** Not enriched; **b** enriched by the magnetic stirrer; **c** enriched by the ultrasonic bath. **d** XRD-scan of one sample from the field for comparison, enriched by the ultrasonic bath. In the model, 6 line ferrihydrite as well as lepidocrocite are found, whereas in the field sample only 6 line ferrihydrite was identified

Table 4 Results of the Rietveld-analysis of one sample from the model (M), either not enriched or enriched by the magnetic stirrer (S) or the ultrasonic bath (U) in comparison to one sample from the field (F), enriched by the ultrasonic bath (U)

Mineral (wt.%)	M	M.S	M.U	F.U
Quartz	95.6	35.1	47.6	27.3
Orthoclase	4.4	12.7	2.7	–
Ferrihydrite 6L	–	39.9	34.9	72.7
Lepidocrocite	–	12.3	14.8	–

the model still differs somewhat from the process in the field. Additional samples are required to assess that aspect.

The laboratory model we used makes it possible to investigate the clogging process with or without several influencing factors. Hence, the clogging tendency can be compared for different combinations of gravel pack materials, well screens, and hydrochemical settings (e.g. input solution on the basis of Fe(II)SO_4). Different ways to regenerate the well screen and gravel pack and the corresponding re-ageing process can also be studied.

Acknowledgments The authors thank Christian Forkel and Wilhelm Schlegel (RWE Power AG) for their cooperation and for creating the unique opportunity to take samples in the open pits. We also thank RWE Power AG for its contribution to the project's funding. Andre Banning (RWTH Aachen University) is acknowledged for his help in analytical and technical questions. Furthermore, we appreciate the inspiring correspondence with Christoph Treskatis (Bieske und Partner Beratende Ingenieure GmbH). Michel Heuser from the Institute of Clay and Interface Mineralogy (CIM) of RWTH Aachen University is acknowledged for allocating the extensive CIM database of structure files and for his assistance in handling the BGMN software. The authors thank Sabine Heim and Katharina Wohlfart of the Institute of Geology and Geochemistry of Petroleum and Coal (LEK) of RWTH Aachen University for their help in sample preparation and for measuring the TOC. David Rubinos from the Departamento de Edafoloxía e Química Agrícola, Facultade de Farmacia, Universidade de Santiago de Compostela and Hui Hu from the Department of Engineering Geology and Hydrogeology (LIH) of RWTH Aachen University are acknowledged for their asistance with the Spanish and Chinese Abstract.

References

Bergmann J, Friedel P, Kleeberg R (1998) BGMN—a new fundamental parameters based Rietveld program for laboratory X-ray sources, its use in quantitative analysis and structure investigations. CPD Newsletter 20:5–8, http://lachlan.bluehaze.com.au/cpdnews98/art05.htm

Childs CW (1992) Ferrihydrite: a review of structure, properties and occurrence in relation to soils. Z Pflanzenernähr Bodenk 155:441–448. doi:10.1002/jpln.19921550515

Cornell RM, Schwertmann U (2003) The iron oxides: structure, properties, reactions, occurences and uses. ISBN 978–3527302741. Wiley-VCH, Weinheim

Davison W, Seed G (1983) The kinetics of the oxidation of ferrous iron in synthetic and natural waters. Geochim Cosmochim Acta 47:67–79. doi:10.1016/0016-7037(83)90091-1

German Institute for Standardization (1983) DIN 38406–1: Deutsche Einheitsverfahren zur Wasser-, Abwasser- und Schlammuntersuchung—Kationen (Gruppe E)—Bestimmung von Eisen (E 1). Beuth, Berlin

German Institute for Standardization (2001) DIN 21919–3: Bergmännisches Risswerk—Stratigraphie—Teil 3: Regionale und lokale Gliederungen Braunkohle. Beuth, Berlin

Hässelbarth U, Lüdemann D (1967) Die biologische Verockerung von Brunnen durch Massenentwicklung von Eisen- und Manganbakterien. BBR 18:363–368, 401–406

Henkel S, Weidner C, Roger S, Schüttrumpf H, Rüde TR, Klauder W, Vinzelberg G (2012) Untersuchung der Verockerungsneigung von Vertikalfilterbrunnen im Modellversuch (Investigation of the clogging affinity of vertical wells using an experimental model). Grundwasser doi: 10.1007/s00767-012-0198-9

Holluta J, Kölle W (1964) Über die Oxydation von zweiwertigem Eisen durch Luftsauerstoff. GWF 105(18):471–474

Houben GJ (2003) Iron oxide incrustations in wells. Part 1: genesis, mineralogy and geochemistry. Appl Geochem 18:927–939. doi:10.1016/S0883-2927(02)00242-1

Houben GJ, Treskatis C (2007) Water well rehabilitation and reconstruction. ISBN 978–0071486514. McGraw-Hill, New York City

Klauder W (2011) Experimental study of flow to vertical groundwater wells. Dissertation, RWTH Aachen University, Germany, http://darwin.bth.rwth-aachen.de/opus3/volltexte/2011/3570/

Ralph DE, Stevenson JM (1995) The role of bacteria in well clogging. Wat Res 29(1):365–369. doi:10.1016/0043-1354(94)E0077-J

Refait P, Génin J-MR (1993) Mechanisms of formation and structure of green rust one in aqueous corrosion of iron in the presence of chloride ions. Corros Sci 40(9):1547–1560. doi:10.1016/S0010-938X(98)00066-3

Rinck-Pfeiffer S, Ragusa S, Sztajnbok P, Vandevelde T (2000) Interrelationships between biological, chemical, and physical processes as an analog to clogging in aquifer storage and recovery (ASR) wells. Wat Res 34(7):2110–2118. doi:10.1016/S0043-1354(99)00356-5

Rüde TR, Banning A, Klauder W, Roger S, Vinzelberg G (2010) Improving the effectiveness of wells for lignite mine dewatering. In: Wolkersdorfer C, Freund A (eds) Mine Water and Innovative Thinking. ISBN 978-1-897009-47-5. CBU Press, Sydney, Nova Scotia, Canada, p 89–93

RWE Power AG (2008) Bericht zur Grundwasserbeschaffenheit—Vorfeld. Bericht 2.4, unpublished

Schneider H, Thiele S (1965) Geohydrologie des Erftgebietes. Ministerium für Ernährung, Landwirtschaft und Forsten des Landes Nordrhein-Westfalen, Aachen

Walter R (2010) Aachen und nördliche Umgebung. Sammlung Geologischer Führer Band 101. ISBN 978-3-443-15087-7 Gebr. Borntraeger, Stuttgart, Germany

Weidner C, Henkel S, Lorke S, Rüde TR, Schüttrumpf H, Klauder W (2011) Investigation of clogging processes on vertical filter wells using an experimental model. In: Rüde TR, Freund A, Wolkersdorfer C (eds) Mine Water—Managing the Challenges. ISBN 978-3-00-035543-1. Comouth, Aachen, p 79–83

Wenzel WW, Kirchbaumer N, Prohaska T, Stingeder G, Lombi E, Adriano DC (2001) Arsenic fractionation in soils using an improved sequential extraction procedure. Anal Chim Acta 436(2):309–323. doi:10.1016/S0003-2670(01)00924-2